

PLY-THICKNESS EFFECT ON FIBER-MATRIX INTERFACE CRACK GROWTH

L. Di Stasio^{1,2}, J. Varna¹, Z. Ayadi²

¹Division of Materials Science, Luleå University of Technology, Luleå, Sweden

²EEIGM & IJL, Université de Lorraine, Nancy, France

9th International Conference on Composite Testing and Model Identification
Luleå (SE), May 27-29, 2019



Outline

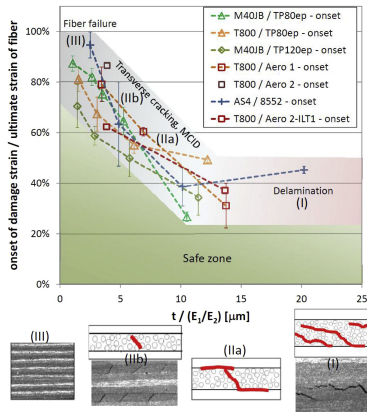
- ➔ Initiation of Transverse Cracks in Thin-plys
- ➔ Modeling the Fiber-Matrix Interface Crack
- ➔ Debond Energy Release Rate
- ➔ Conclusions



INITIATION OF TRANSVERSE CRACKS IN THIN-PLIES

The Thin-ply "Advantage": new material

2018, $[45^\circ, 90^\circ, -45^\circ, 0]$ ns

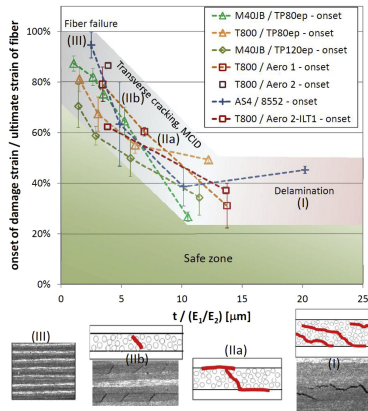


Cugnoni et al., Compos. Sci. Technol. **168**, 2018, p. 467–477.

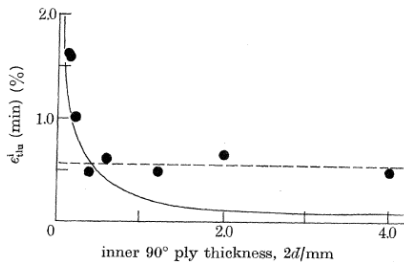
The Thin-ply "Advantage": new material, old result

2018, $[45^\circ, 90^\circ, -45^\circ, 0]_{ns}$

1979, $[0^\circ, 90^\circ]_s$

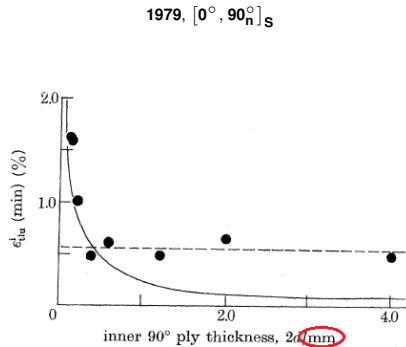
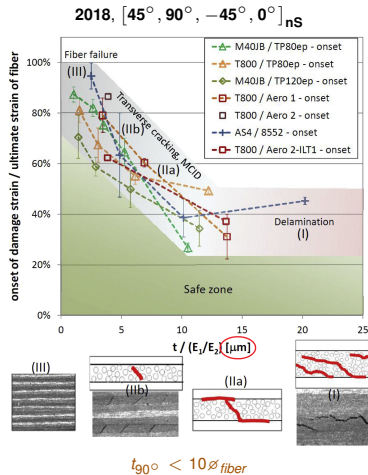


Cugnoni et al., Compos. Sci. Technol. **168**, 2018, p. 467–477.



Bailey et al., P. Roy. Soc. A-Math. Phys. **366** (1727), 1979.

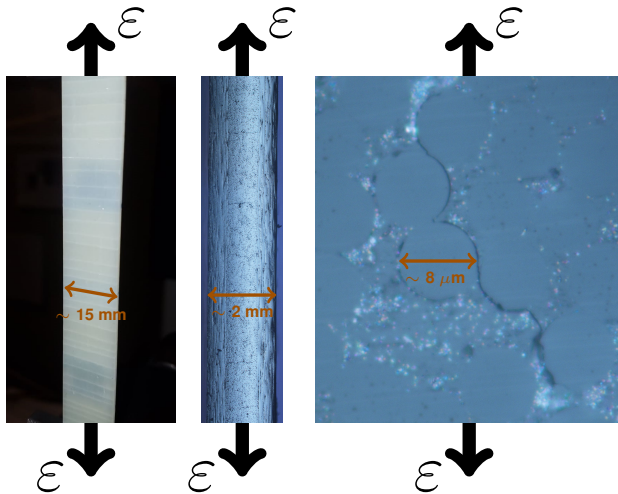
The Thin-ply "Advantage": new material, old result?



Cugnoni et al., Compos. Sci. Technol. **168**, 2018.

Bailey et al., P. Roy. Soc. A-Math. Phys. **366** (1727), 1979.

Micromechanics of Initiation



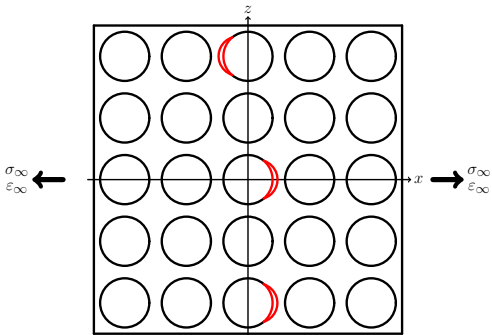
Left:
front view of $[0, 90]_S$,
visual inspection.

Center:
edge view of $[0, 90]_S$,
optical microscope.

Right:
edge view of $[0, 90]_S$,
optical microscope.

Micromechanics of Initiation

Stage 1: isolated debonds



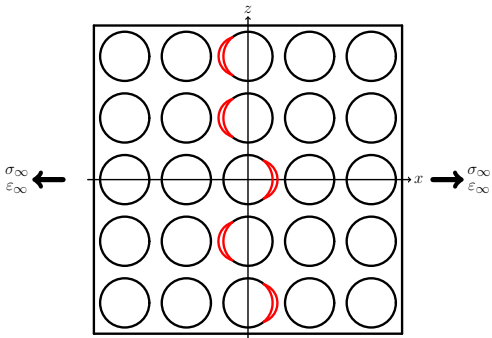
Bailey et al., P. Roy. Soc. A-Math. Phy. **366** (1727), 1979.

Bailey et al., J. Mater. Sci. **16** (3), 1981.

Zhang et al., Compos. Part A-Appl. S. **28** (4), 1997.

Micromechanics of Initiation

Stage 2: consecutive debonds



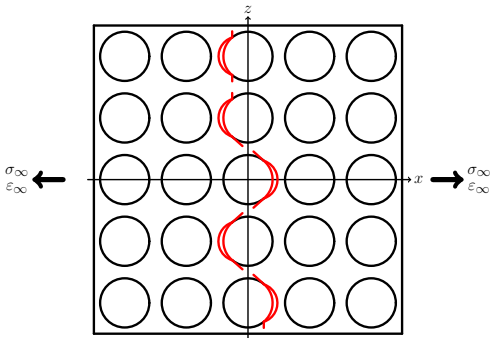
Bailey et al., P. Roy. Soc. A-Math. Phy. **366** (1727), 1979.

Bailey et al., J. Mater. Sci. **16** (3), 1981.

Zhang et al., Compos. Part A-Appl. S. **28** (4), 1997.

Micromechanics of Initiation

Stage 3: kinking



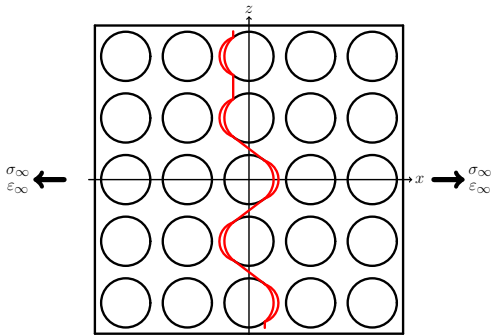
Bailey et al., P. Roy. Soc. A-Math. Phy. **366** (1727), 1979.

Bailey et al., J. Mater. Sci. **16** (3), 1981.

Zhang et al., Compos. Part A-Appl. S. **28** (4), 1997.

Micromechanics of Initiation

Stage 4: coalescence



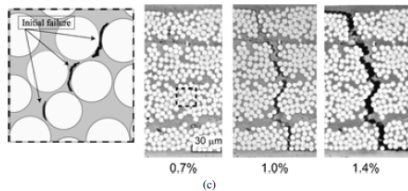
Bailey et al., P. Roy. Soc. A-Math. Phy. **366** (1727), 1979.

Bailey et al., J. Mater. Sci. **16** (3), 1981.

Zhang et al., Compos. Part A-Appl. S. **28** (4), 1997.

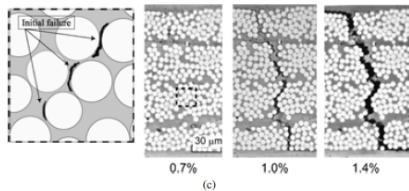
A Counter-intuitive Observation

$[0^\circ, 90_n^\circ]_S$

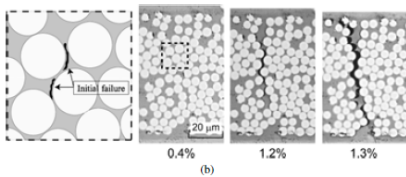


A Counter-intuitive Observation

$[0^\circ, 90_n^\circ]_S$



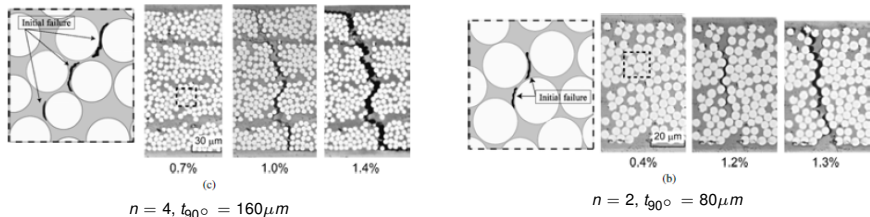
$$n = 4, t_{90^\circ} = 160 \mu\text{m}$$



$$n = 2, t_{90^\circ} = 80 \mu\text{m}$$

A Counter-intuitive Observation

$[0^\circ, 90^\circ]_S$

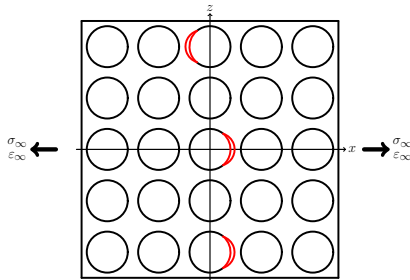


Saito et al., Adv. Compos. Mater. 21 (1), 2012.

Objective of the Study

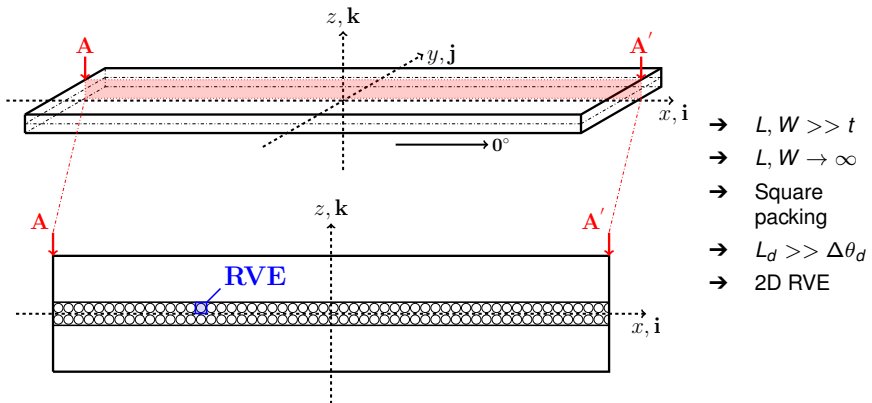
Can we talk about a ply-thickness effect for the fiber-matrix interface crack?

Stage 1: isolated debonds

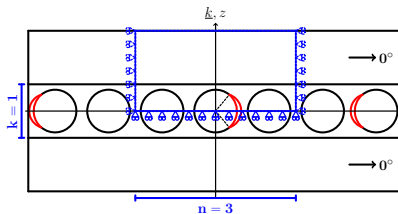


MODELING THE FIBER-MATRIX INTERFACE CRACK

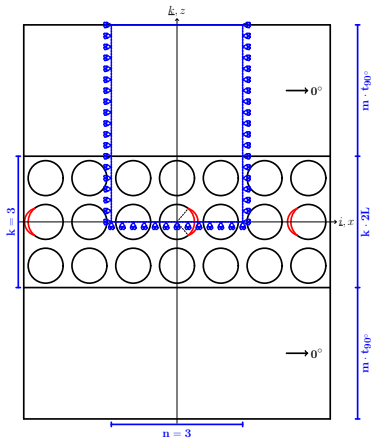
Geometry



Representative Volume Elements

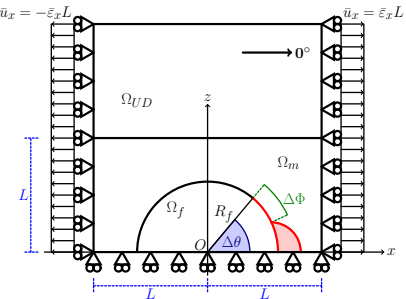


$$n \times 1 - m \cdot t_{90^\circ}$$



$$n \times k - m \cdot t_{90^\circ}$$

Assumptions

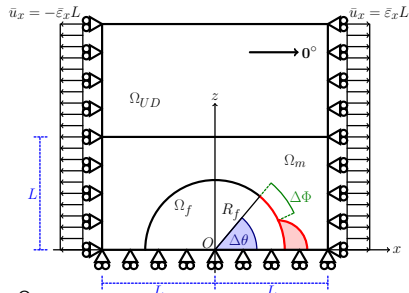


- Linear elastic, homogeneous materials
- Concentric Cylinders Assembly with Self-Consistent Shear Model for UD
- Plane strain
- Frictionless contact interaction
- Symmetric w.r.t. x-axis
- Coupling of x-displacements on left and right side (repeating unit cell)
- Applied uniaxial tensile strain $\bar{\varepsilon}_x = 1\%$
- $V_f = 60\%$

$$R_f = 1 \text{ } [\mu\text{m}] \quad L = \frac{R_f}{2} \sqrt{\frac{\pi}{V_f}}$$

Material	V_f [%]	E_L [GPa]	E_T [GPa]	μ_{LT} [GPa]	ν_{LT} [-]	ν_{TT} [-]
Glass fiber	-	70.0	70.0	29.2	0.2	0.2
Epoxy	-	3.5	3.5	1.25	0.4	0.4
UD	60.0	43.442	13.714	4.315	0.273	0.465

Solution



in Ω_f , Ω_m , Ω_{UD} :

$$\frac{\partial^2 \varepsilon_{xx}}{\partial z^2} + \frac{\partial^2 \varepsilon_{zz}}{\partial x^2} = \frac{\partial^2 \gamma_{zx}}{\partial x \partial z} \quad \text{for } 0^\circ \leq \alpha \leq \Delta\theta : \quad (\vec{U}_m(R_f, \alpha) - \vec{U}_f(R_f, \alpha)) \cdot \vec{n}_\alpha \geq 0$$

$$\varepsilon_y = \gamma_{xy} = \gamma_{yz} = 0$$

$$\frac{\partial \sigma_{xx}}{\partial x} + \frac{\partial \tau_{zx}}{\partial z} = 0 \quad \text{for } \Delta\theta \leq \alpha \leq 180^\circ : \quad \vec{U}_m(R_f, \alpha) - \vec{U}_f(R_f, \alpha) = 0$$

$$\frac{\partial \tau_{zx}}{\partial x} + \frac{\partial \sigma_{zz}}{\partial z} = 0 \quad \sigma_{ij} = E_{ijkl} \varepsilon_{kl}$$

$$\sigma_{yy} = \nu (\sigma_{xx} + \sigma_{zz})$$

→ Oscillating singularity

$$\sigma \sim r^{-\frac{1}{2}} \sin(\varepsilon \log r), \quad V_f \rightarrow 0$$

$$\varepsilon = \frac{1}{2\pi} \log \left(\frac{1-\beta}{1+\beta} \right)$$

$$\beta = \frac{\mu_2(\kappa_1 - 1) - \mu_1(\kappa_2 - 1)}{\mu_2(\kappa_1 + 1) + \mu_1(\kappa_2 + 1)}$$

$$\rightarrow G = \frac{\partial W}{\partial A} - \left(\frac{\partial U}{\partial A} + \frac{\partial E_k}{\partial A} \right)$$

→ Finite Element Method (FEM)
in Abaqus™

→ 2nd order shape functions

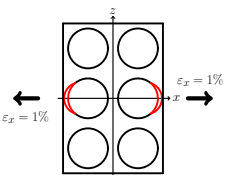
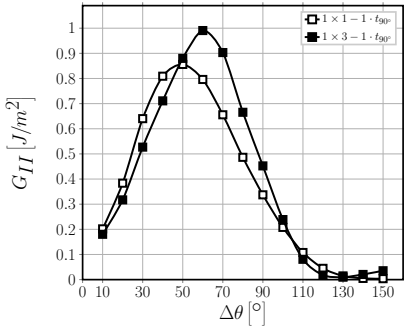
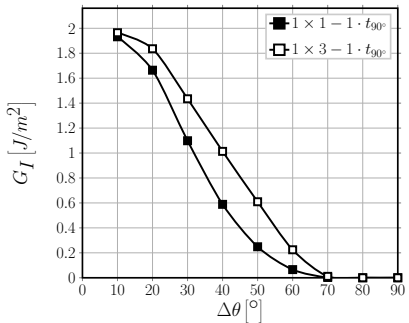
→ 6-nodes triangles & 8-nodes quadrilaterals

→ regular mesh of quadrilaterals
at the crack tip:

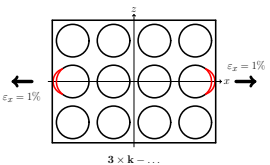
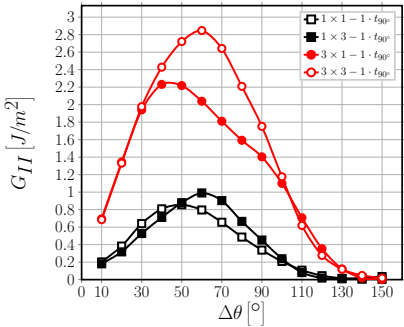
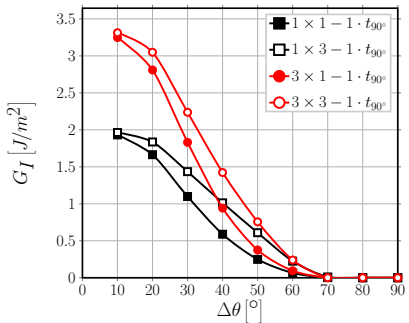
- $AR \sim 1$
- $\delta = 0.05^\circ$

DEBOND ENERGY RELEASE RATE

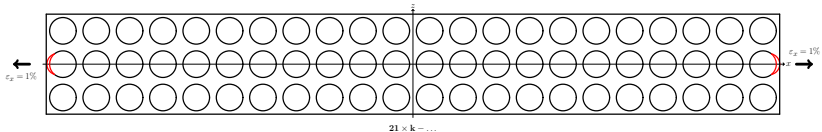
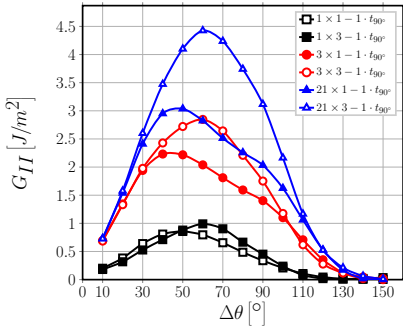
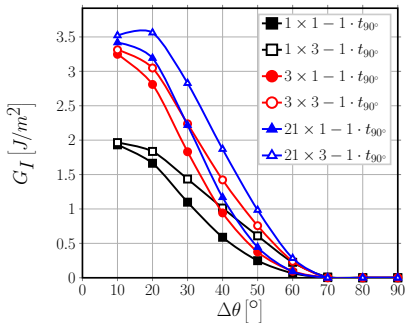
Interaction of Debonds: Strain Magnification



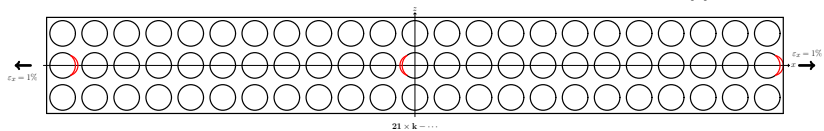
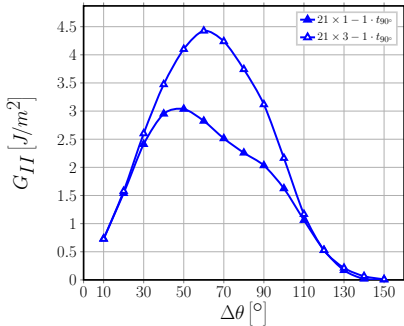
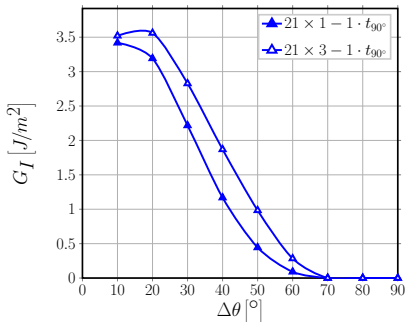
Interaction of Debonds: Strain Magnification



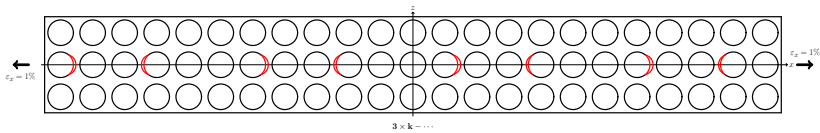
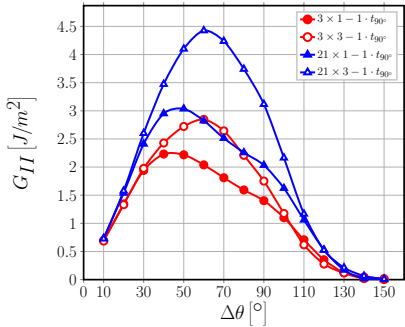
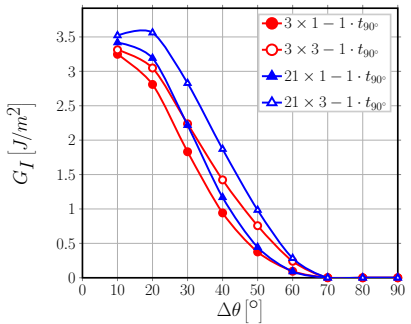
Interaction of Debonds: Strain Magnification



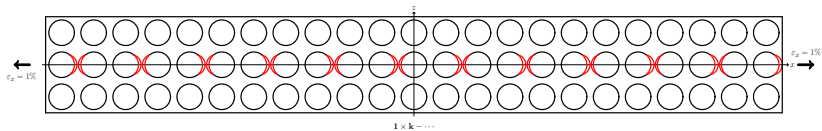
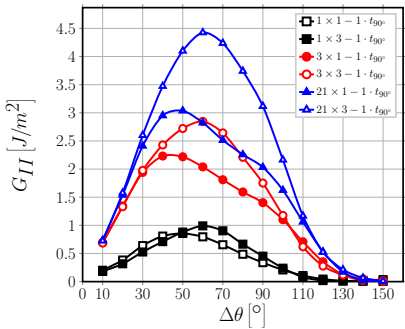
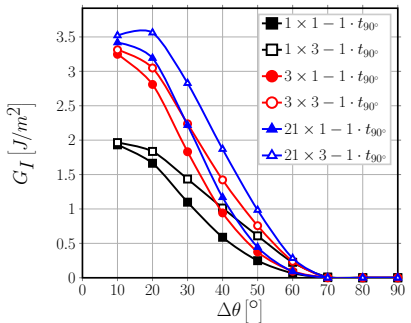
Interaction of Debonds: Crack Shielding



Interaction of Debonds: Crack Shielding



Interaction of Debonds: Crack Shielding



CONCLUSIONS

Conclusions

- Debond-debond interaction in the through-the-thickness direction is extremely localized: with only a couple of undamaged fibers in between, no effect can be seen!
- For debonds on consecutive vertically-aligned fibers, G_{II} is higher and contact zone onset delayed if debonds are on the same side of their respective fiber.
- No significant difference in G_{II} observed, except in the range $80^\circ - 100^\circ$.
- In the range $80^\circ - 100^\circ$, G_{II} is higher when debonds are located on opposite sides of consecutive vertically-aligned fibers.



LULEÅ
UNIVERSITY
OF TECHNOLOGY



Education and Culture

Erasmus Mundus